

Electrical Field Shaping Techniques in a Feline Model of Retinal Degeneration*

Thomas C. Spencer, James B. Fallon, *Member, IEEE*, Carla J. Abbott, Penny J. Allen, Alice Brandli, Chi D. Luu, Stephanie B. Epp and Mohit N. Shivdasani, *Senior Member, IEEE***

Abstract— The majority of preclinical studies investigating multi-electrode field shaping stimulation strategies for retinal prostheses, have been conducted in normally-sighted animals. This study aimed to reassess the effectiveness of two electrical field shaping techniques that have been shown to work in healthy retinæ, in a more clinically relevant animal model of photoreceptor degeneration. Four cats were unilaterally blinded via intravitreal injections of adenosine triphosphate. Cortical responses to traditional monopolar (MP) stimulation, focused multipolar (FMP) stimulation and two-dimensional current steering were recorded. Contrary to our previous work, we found no significant difference between the spread of cortical activation elicited by FMP and MP stimulation, and we were not able to reproduce cortical responses to single-electrode retinal stimulation using two-dimensional current steering. These findings suggest that while shown to be effective in normally-sighted animals, these techniques may not be readily translatable to patients with retinal degeneration and require further optimization.

I. INTRODUCTION

Electrical field shaping techniques have shown significant promise in recent years in terms of increasing the resolution of neural prosthetic devices constrained by surgical and engineering limitations [1–5]. Techniques such as current focusing and current steering employ simultaneous stimulation of multiple electrodes with the purpose of either sharpening or shifting the focus of the resultant electric field, respectively. Clinical success of these strategies in patients fitted with cochlear and deep brain stimulation implants has been varied [6–10]. In the field of retinal prosthetics to date, our group [3,4,11] and others [1,2,12,13] have shown promising results using these methods in normal-sighted animal models. However, it is well known that inherited dystrophies such as retinitis pigmentosa, the main target disease for retinal implants, cause significant remodeling events in the retina and central visual pathway as a result of photoreceptor death [14,15]. *A priori*, one would expect that

these changes would compromise the effectiveness of retinal stimulation.

The disparity between the typical model used in the development of retinal prostheses and the nature of the disease state they are intended to treat, makes it difficult to draw reliable translational conclusions from preclinical studies. In our previous work, we have detailed the development of a cat model of long-term retinal degeneration using intravitreal injections of adenosine triphosphate (ATP) to induce photoreceptor death, leading to significant remodeling of the inner retina in some cases [16,17]. Comparative electrophysiological studies by our group in these animals have shown significant differences in cortical responses to electrical stimulation of healthy versus degenerated retinæ, such as increased activation thresholds, increased size of cortical receptive fields, and lower saturated spike counts [18,19].

The aim of this study is therefore to reevaluate the effectiveness of two electrical field shaping techniques that we have investigated in past years in normal-sighted retinæ. Focused multipolar (FMP) stimulation is a technique that aims to spatially restrict the electric field [20]. We have shown FMP stimulation to be effective in reducing the spread of retinal and cortical activation compared to monopolar (MP) stimulation [3]. We have also demonstrated the potential of current steering in the retina to shift the peak of an electric field, creating “virtual electrodes” and allowing us to target specific neural populations that may otherwise be unreachable using single electrodes [5,11].

II. METHODS

A. Ethics Statement

All procedures were approved by the Bionics Institute Animal Research Ethics Committee (Project #14 304AB) and were in accordance with the Australian Code of Practice for the Care Use of Animals for Scientific Purposes (8th edition).

B. Unilateral Blinding Procedure

Four domestic cats were anesthetized with ketamine (intramuscular [i.m.], 20 mg/kg) and xylazil (subcutaneous [s.c.], 2 mg/kg). A 200 μ L solution of three parts sterile saline (0.9% NaCl) and one part Dexamethasone (4 mg/mL), containing approximately 0.2 M (11 mM vitreous concentration) ATP disodium salt (Sigma-Aldrich Corp., St. Louis, MO, USA) was injected into the intravitreal space of one eye. Following a two-week recovery period, the

*Research supported by National Health and Medical Research Council (NHMRC; GNT#1063093); **Corresponding Author.

T. C. Spencer, J. B. Fallon and S.B. Epp are with the Bionics Institute and the Department of Medical Bionics, University of Melbourne, East Melbourne, Australia.

C. J. Abbott, P. J. Allen, A. Brandli, and C. D. Luu are with the Centre for Eye Research Australia and the Department of Surgery (Ophthalmology), East Melbourne, Australia.

M. N. Shivdasani was with the Bionics Institute, East Melbourne, Australia. He is now with the Graduate School of Biomedical Engineering, University of New South Wales, Sydney, Australia (Phone: +61 401 311 423; e-mail: m.shivdasani@unsw.edu.au).

structure and function of the retina was assessed under anesthesia and compared with baseline measurements recorded prior to the injection. We considered a 50% reduction in the a-wave amplitude of a dark-adapted electroretinogram, and significant retinal thinning beneath the area centralis (as judged using fundus photography and optical coherence tomography), to be our minimum threshold for significant photoreceptor loss. If these criteria were not met, a second ATP injection was given [18,19].

C. Surgical Procedure

Fourteen weeks following the observation of significant retinal degeneration, cats were anesthetized with ketamine (i.m. 8 mg/kg), medetomidine (i.m. 0.012 mg/kg), and methadone (i.m. 0.4 mg/kg). Anesthesia was maintained through a continuous intravenous infusion of Propofol (24 mg/kg). Tracheostomies were performed and the animals ventilated on 100% oxygen (20-25 breaths/min; Model 6025; Ugo Basile, Monvalle, VA, Italy). A 42-channel platinum electrode array was implanted into the suprachoroidal space of each eye with the array tip beneath the area centralis [21]. Bilateral craniotomies were performed, exposing the visual cortices (VC). Following removal of the dura mater, 6x10 planar electrode arrays (Blackrock Microsystems, Foxborough, MA, USA) were inserted to a depth of ~1 mm in the regions of the VC with the lowest evoked potential thresholds to retinal stimulation of each eye (measured using non-invasive surface electrodes).

D. Stimulation paradigms

Electrical stimuli were generated with a 128-channel IZ2 stimulator (Tucker-Davis Technologies, Alachua, FL, USA). Symmetric biphasic pulses (1000 μ s phase width and 25 μ s interphase gap) were presented to the retinal arrays against a remote extraocular platinum return, at randomly varied currents ranging from 0-750 μ A in 50 μ A steps (10 repeats each) at a repetition rate of 1 Hz [3].

Initially, cortical responses to MP stimulation (Figure 1a) of each retinal electrode were recorded to provide comparisons to the FMP and steered stimuli to follow. Transimpedance measurements were taken using custom

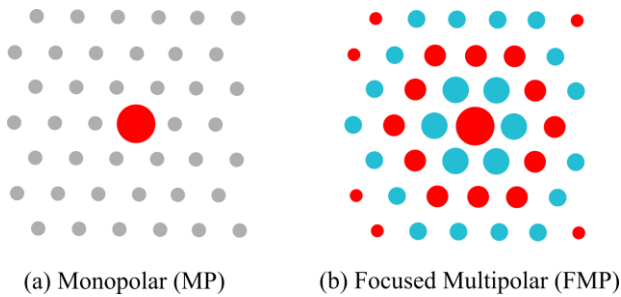


Figure 1. Illustration of electrode stimuli weights for MP and FMP stimulation techniques. MP stimulation is represented as a single stimulating electrode. FMP weights typically present as concentric rings of alternating positive and negative currents, producing a focused electrical field at the site of the central electrode.

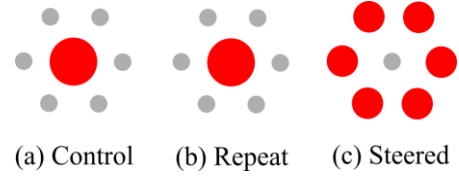


Figure 2. Illustration of the steered stimulation configurations used in this study. Note that the total charge delivered when using all stimulation modes was kept the same.

software written in LabVIEW (National Instruments, Austin, TX). Using these measurements, FMP weights were calculated in the same manner as described in Spencer et al, 2016 [3]. FMP stimulation was then applied to the retina (Figure 1b). In a second protocol, we compared cortical responses to MP stimulation with that of two-dimensional steering. Figure 2 shows the different terms used to describe stimuli with respect to a control stimulus on a single central electrode. Repeat stimulation is where we stimulated the same electrode as the control with identical stimulus parameters, in order to assess the average degree of inherent variation in the cortical response to repeated stimulation. This was then compared to responses to steered stimulation, whereby the 6 electrodes surrounding the central electrode each received an equal one-sixth of charge, with the intention of creating a virtual electrode between them. For both repeat and steered stimulation, the shift in the centroid of cortical activity from stimulation of the control electrode was calculated. Based on our previous results in normal retinæ [5], we expected that steered stimulation would produce a similar cortical centroid shift than that produced by repeated stimulation of the central electrode.

E. Data analysis

Cortical recordings were analyzed using custom scripts written in Igor Pro (Wavemetrics, Lake Oswego, OR, USA) and MATLAB (Mathworks, Natick, MA, USA). Following artefact removal and bandpass filtering (0.3-5 kHz), spikes were timestamped when the signal exceeded 4 times the root mean square value. Spikes corresponding to both direct activation of RGCs and indirect activation of the network [3-5,11,18,19] were detected and analyzed within a 3-20 ms window post-stimulus after subtracting any spontaneous activity. For each recording channel, spike rates averaged across the 10 repetitions of each current step were used to construct an input-output function.

Threshold for each recording channel was defined as the lowest current required to exhibit spike rates greater than that evoked by a zero current while showing a monotonic increase in spiking activity at all higher current levels. The spread of cortical activation was measured using the same technique as outlined in Spencer et al 2016 using a discriminability index measure [3]. For each stimulus, the recording channel with the least charge required to reach a d' of 1 was designated the best cortical electrode (BCE). The average d' calculated for other recording channels at the charge that elicited a d' value of 1 on the BCE was then

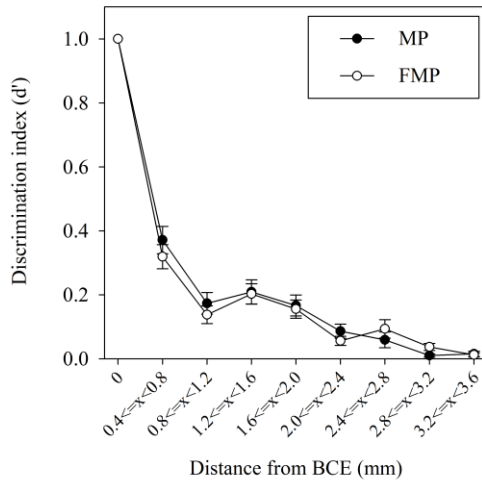


Figure 3. Average of the maximum d' values of cortical channels at the current required to reach $d'=1$ above threshold on the BCE for each stimulation mode. No significant difference between the two stimulation modes were observed ($p>0.05$, two-way RM ANOVA), indicating no difference in the spread of cortical activation..

plotted as a function of distance from BCE (Figure 3). A steeper drop in the d' value indicated a reduced spread of activation [3]. For steering analyses, a sigmoid curve was fitted to each IO function. A P90 current level was calculated as the point at which the sigmoid curve reached 90% of the maximum saturated spike rate on a recording channel. Spatial activation maps across the recording array were constructed at the P90 current level of the lowest threshold recording electrode. The shift in the centroids of the cortical spatial maps from the centroid obtained with the control stimulus was compared between the repeat and steered stimulation paradigms [5,11].

III. RESULTS

In all four animals, significant degeneration of the outer nuclear layer was observed above the region where the stimulating arrays were implanted. Results of the clinical data have been recently published [19].

A. Focused Multipolar Stimulation

Cortical responses were collected in response to MP and FMP stimulation of 139 retinal electrodes across all 4 animals. Consistent with our previous work [3], FMP stimulation showed significantly higher cortical thresholds compared to MP stimulation ($p<0.001$, paired t-test). Out of the 139 retinal electrodes stimulated, only the 53 electrodes where spiking on at least one cortical channel reached a d' value of 1 above threshold using both MP and FMP stimulation were included in the spread analysis. No significant difference in cortical spread was observed between MP and FMP stimulation ($p>0.05$ two-way ANOVA).

B. Virtual Electrode Stimulation

Cortical centroid shifts from the centroid obtained by stimulating a control electrode could be calculated for

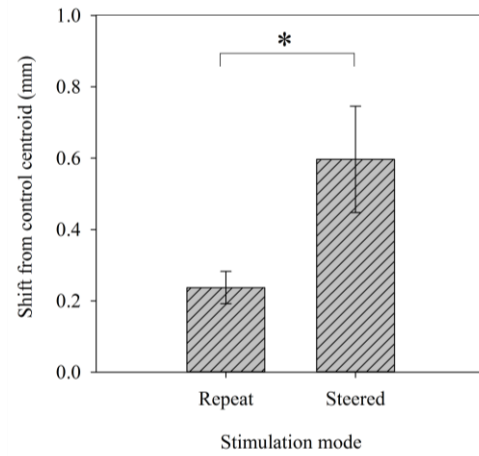


Figure 4. Bar chart showing the average shift in the centroid of activation obtained for repeat ($n=23$) and steered ($n=11$) relative to the centroid obtained with the control paradigm. Asterisk denotes a significant difference between the two stimulation modes (one-tailed t-test, $p<0.005$).

stimulation of 23 repeat and 11 steered electrodes. As shown in Figure 4, steered electrodes elicited a significantly greater ($p<0.005$, t-test) shift in cortical centroid than repeat electrodes, indicating that a virtual electrode identical to the central electrode had not been created.

IV. DISCUSSION

Contrary to our previous study in normal-sighted animals, FMP stimulation of the blind retina was found to show no significant reduction in the spread of cortical activity when compared to MP stimulation. In addition to this and more unexpectedly, it was found that MP stimulation of the degenerated retinæ in this study resulted in even lower spread than when stimulating healthy retinæ reported in our previous study [3]. However, it should be noted that statistical comparisons made between MP and FMP stimulation were always paired in order to account for differences in the cortical magnification factor at different degrees of retinal eccentricity. Direct comparison between eyes do not account for this. With regards to current steering in degenerate retinæ, steered electrodes produced “different” responses to central electrodes, opposite to what we previously reported in healthy retinæ [5,11].

These results indicate that despite promising preclinical results for FMP and current steering in normal-sighted animals, these techniques in their present form may not be effective in patients with degenerated retinæ. Our previous work has shown that stimulation of degenerated retinæ elicits responses with significantly increased activation thresholds and cortical receptive fields [18,19]. These changes, coupled with other unexplored retinal and cortical remodeling may have a significant impact on the spatial properties of the response to electrical stimulation. Further clinical, histological and immunohistochemistry analyses of the retina, particularly correlations between the extent of degeneration/remodeling and the effectiveness of current

steering and focusing, are expected to provide a deeper insight in to the reasons behind these unexpected results. Ultimately, it is envisaged that field shaping paradigms will need to be further optimized in order to provide higher spatial resolution in blind retinæ.

V. CONCLUSION

This study showed that electrical field shaping techniques proven to be effective in normal healthy retinæ are ineffective when applied to degenerate retinæ. It also provides further evidence that the responses of degenerated retinæ to electrical stimulation are significantly different to that of healthy retinæ. These findings give greater weight to the argument that further optimization of stimulation strategies will need to be carried out in models that closer represent the physiology of patients with retinal degeneration in order to better inform translational endeavors.

ACKNOWLEDGMENT

The authors wish to thank Ceara McGowan, Ali Almasi, Felix Aplin, Kerry Halupka, Faith Lamont, Rodney Millard, Alison Neil, Alexia Saunders, Evgeni Sergeev, Dimitra Stathopoulos, and Patrick Thien for technical assistance. Funding was provided by the National Health and Medical Research Council (NHMRC) Project Grant #1063093. The Bionics Institute acknowledges the support it receives from the Victorian Government through its Operational Infrastructure Support Program.

REFERENCES

- [1] Habib A G, Cameron M a, Suaning G J, Lovell N H and Morley J W 2013 Spatially restricted electrical activation of retinal ganglion cells in the rabbit retina by hexapolar electrode return configuration. *J. Neural Eng.* **10** 36013
- [2] Matteucci P B, Chen S C, Tsai D, Dodds C W D, Dokos S, Morley J W, Lovell N H and Suaning G J 2013 Current steering in retinal stimulation via a quasimonopolar stimulation paradigm. *Invest. Ophthalmol. Vis. Sci.* **54** 4307–20
- [3] Spencer T C, Fallon J B, Thien P C and Shivdasani M N 2016 Spatial restriction of neural activation using focused multipolar stimulation with a retinal prosthesis *Invest. Ophthalmol. Vis. Sci.* **57** 3181–91
- [4] Halupka K J, Shivdasani M N, Cloherty S L, Grayden D B, Wong Y T, Burkitt A N and Meffin H 2017 Prediction of cortical responses to simultaneous electrical stimulation of the retina *J. Neural Eng.* **14** 016006
- [5] Spencer T C, Fallon J B and Shivdasani M N 2018 Creating virtual electrodes with two-dimensional current steering *J. Neural Eng.* **15** 035002
- [6] Koch D B, Downing M, Osberger M J and Litvak L 2007 Using current steering to increase spectral resolution in CII and HiRes 90K users. *Ear Hear.* **28** 38S–41S
- [7] Firszt J B, Koch D B, Downing M and Litvak L 2007 Current steering creates additional pitch percepts in adult cochlear implant recipients. *Otol. Neurotol.* **28** 629–36
- [8] Barbe M T, Maarouf M, Alesch F and Timmermann L 2014 Multiple source current steering - a novel deep brain stimulation concept for customized programming in a Parkinson's disease patient *Park. Relat. Disord.* **20** 471–3
- [9] Smith Z M, Parkinson W S and Long C J 2013 Multipolar current focusing increases spectral resolution in cochlear implants *Proc. Annu. Int. Conf. IEEE Eng. Med. Biol. Soc. EMBS* 2796–9
- [10] Landsberger D M and Srinivasan A G 2009 Virtual channel discrimination is improved by current focusing in cochlear implant recipients *Hear. Res.* **254** 34–41
- [11] Dumm G, Fallon J B, Williams C E and Shivdasani M N 2014 Virtual electrodes by current steering in retinal prostheses *Invest. Ophthalmol. Vis. Sci.* **55** 8077–85
- [12] Jepson L H, Hottowy P, Mathieson K, Gunning D E, Dąbrowski W, Litke A M and Chichilnisky E J 2014 Spatially patterned electrical stimulation to enhance resolution of retinal prostheses. *J. Neurosci.* **34** 4871–81
- [13] Eiber C D, Dokos S, Lovell N H and Suaning G J 2017 Multipolar field shaping in a suprachoroidal visual prosthesis *IEEE Trans. Neural Syst. Rehabil. Eng.* **25** 2480–87
- [14] Marc R E, Jones B W, Watt C B and Strettoi E 2003 Neural remodeling in retinal degeneration *Prog. Retin. Eye Res.* **22** 607–55
- [15] Jones B W and Marc R E 2005 Retinal remodeling during retinal degeneration. *Exp. Eye Res.* **81** 123–37
- [16] Aplin F P, Luu C D, Vessey K a., Guymer R H, Shepherd R K and Fletcher E L 2014 ATP-Induced Photoreceptor Death in a Feline Model of Retinal Degeneration *Invest. Ophthalmol. Vis. Sci.* **55** 8319–29
- [17] Aplin F P, Vessey K A, Luu C D, Guymer R H, Shepherd R K and Fletcher E L 2016 Retinal Changes in an ATP-Induced Model of Retinal Degeneration *Front. Neuroanat.* **10** 1–13
- [18] Aplin F P, Fletcher E L, Luu C D, Vessey K A, Allen P J, Guymer R H, Shepherd R K and Shivdasani M N 2016 Stimulation of a suprachoroidal retinal prosthesis drives cortical responses in a feline model of retinal degeneration *Invest. Ophthalmol. Vis. Sci.* **57** 5216–29
- [19] Halupka K J, Abbott C J, Wong Y T, Cloherty S L, Grayden D B, Burkitt A N, Sergeev E N, Luu C D, Brandli A, Allen P J, Meffin H and Shivdasani M N 2017 Neural Responses to Multielectrode Stimulation of Healthy and Degenerate Retina *Invest. Ophthalmol. Vis. Sci.* **58** 3770–84
- [20] van den Honert C and Kelsall D C 2007 Focused intracochlear electric stimulation with phased array channels. *J. Acoust. Soc. Am.* **121** 3703–16
- [21] Villalobos J, Allen P J, McCombe M F, Ulaganathan M, Zamir E, Ng D C, Shepherd R K and Williams C E 2012 Development of a surgical approach for a wide-view suprachoroidal retinal prosthesis: evaluation of implantation trauma. *Graefes Arch. Clin. Exp. Ophthalmol.* **250** 399–407